Research Article

Rapid Communications in Mass Spectrometry

Received: 4 September 2010 Revised: 25 December 2010 Accepted: 27 December 2010 Published online in Wiley Online Library: 2011

Rapid Commun. Mass Spectrom. **2011**, *25*, 719–730
(wileyonlinelibrary.com) DOI: 10.1002/rcm.4922

Characterization of metabolism of (+)-praeruptorin B and (+)-praeruptorin E in human and rat liver microsomes by liquid chromatography coupled with ion trap mass spectrometry and time-of-flight mass spectrometry

Yue-Lin Song[1], Ru Yan[1]*, Wang-Hui Jing[1], Hai-Yu Zhao[1] and Yi-Tao Wang[1,2]*

[1]Institute of Chinese Medical Sciences, University of Macau, Taipa, Macao, China
[2]School of Chinese Materia Medica, Beijing University of Chinese Medicine, Beijing, China

Peucedani Radix is a Chinese medicinal herb noted for its effects on treatments of respiratory and pulmonary disorders. As a part of a systematic pharmacokinetic evaluation of the herb in our laboratory, the present study investigated, for the first time, the metabolic profile of (+)-praeruptorin B (*d*PB) and (+)-praeruptorin E (*d*PE), two main bioactive constituents of Peucedani Radix in pooled liver microsomes of rats (RLMs) and humans (HLMs). *d*PE was eliminated faster than *d*PB in both species. The incubation of *d*PB with RLMs and HLMs resulted in eight (B1–B8) and nine (B1–B9) metabolites, respectively, while both RLMs and HLMs converted *d*PE into 13 metabolites (E1–13). Structures of all the metabolites were proposed through comparing their mass data obtained via tandem mass spectrometry on an MSD ion trap system (IT-MS/MS) coupled with high-resolution mass measurement by time-of-flight mass spectrometry (TOF-MS) with those of the respective parent compound. B1 and E1 were unambiguously identified as (−)-*cis*-khellactone. The formations of all the metabolites were NADPH-dependent. Oxidation and hydrolysis were demonstrated to be two predominant metabolic pathways of *d*PB and *d*PE. Oxidation initiated at either the C-3′ or C-4′ substituent, while hydrolysis only started from the C-3′ substituent. Fragmentation of all metabolites followed similar pathways to those of the parent pyranocoumarins. The information on metabolic properties of *d*PB and *d*PE and the mass fragmentation profiles of their metabolites obtained in the present study will aid in characterization of metabolic profiles of other angular-type pyranocoumarins and further investigation of *in vivo* fates of these pyranocoumarins and the herb. Copyright © 2011 John Wiley & Sons, Ltd.

Peucedani Radix (Chinese name Qian-hu), the dried roots of *Peucedanum praeruptorum* Dunn (Apiaceae), is a herbal medicine noted for its cough-relieving and sputum-reducing effects and has been traditionally utilized as antitussive and mucolytic agents for centuries in China.[1] In addition to the well-known actions on respiratory disorders, modern pharmacologic evaluation of Peucedani Radix also revealed significant beneficial effects of the herb on pulmonary hypertension in animal models[2–4] and patients.[5,6]

So far, more than 50 coumarins have been isolated from Peucedani Radix, including (±)-praeruptorin A, (±)-praeruptorin B, (+)-praeruptorin A, (+)-praeruptorin B, (+)-praeruptorin E, etc.[7–10] Most of these coumarins belong to angular-type pyranocoumarin, which has a khellactone skeleton with different substituents at the C-3′ and C-4′ positions. Numerous pharmacologic studies have been carried out on *in vitro* and *in vivo* models and demonstrated diverse biological activities of these pyranocoumarins, including anti-asthma, vasorelaxant, cardiac protective, hepatoprotective, anti-tumor and anti-platelet aggregation activities.[11–16]

In contrast to extensive pharmacologic studies, the pharmacokinetic properties including the metabolism of the coumarin constituents of Peucedani Radix have scarcely been reported, hence their contribution to the herbal activities and *in vivo* active forms remain unclear. As a part of an ongoing project on systematic pharmacokinetic evaluation of Peucedani Radix in our laboratory, metabolic profiling of the main angular-type pyranocoumarins in rat liver microsomes was carried out to aid their correlation in the *in vivo* fates of the main constituents with the reported beneficial actions of the herb on the rat. Further, the metabolic properties of the compounds in human liver microsomes were characterized in parallel to determine whether the data obtained from the rat are extrapolative to humans.

High-performance liquid chromatography/ion trap tandem mass spectrometry (HPLC/IT-MS/MS) is a sensitive and versatile analytical system that applies the ion trap technique to identify both large and small molecules from complex biological systems. The advantages of IT-MS/MS lie in the ability to perform multiple stages of mass spectrometry (MS^n) to facilitate sensitive and specific structural identification.[17] In comparison, HPLC coupled with time-of-flight mass spectrometry (HPLC/TOF-MS) uses the differences in

* *Correspondence to*: R. Yan or Y.-T. Wang, Institute of Chinese Medical Sciences, University of Macau, Macao SAR, China. E-mail: ruyan@umac.mo; ytwang@umac.mo

transit time through a drift region to separate ions of different masses, thus can provide accurate mass weight and the molecular formula of the analyte to assist structural identification.[18] IT-MS/MS and TOF-MS have been widely adopted in combination to characterize metabolites in biological materials.

(+)-Praeruptorin B (*d*PB, Fig. 1) and (+)-praeruptorin E (*d*PE, Fig. 2), the two main angular-type pyranocoumarins in Peucedani Radix, have exhibited anti-tumor and calcium channel antagonistic activities and were considered to contribute to the herbal activities.[19,20] The only structural difference between these two compounds is the substituent at the 4′ position: it is an angeloyl group in *d*PB yet an isovaleryl group in *d*PE. In the present study, the metabolic profiles of *d*PB and *d*PE in rat and human liver microsomes were investigated, for the first time, to find out whether this structural difference results in distinct metabolic profiles. The main focus of the study was on the elucidation of metabolic pathways of *d*PB and *d*PE using HPLC/IT-MS/MS and HPLC/TOF-MS and characterization of the metabolic difference between the two compounds and the species difference between rats and humans if any.

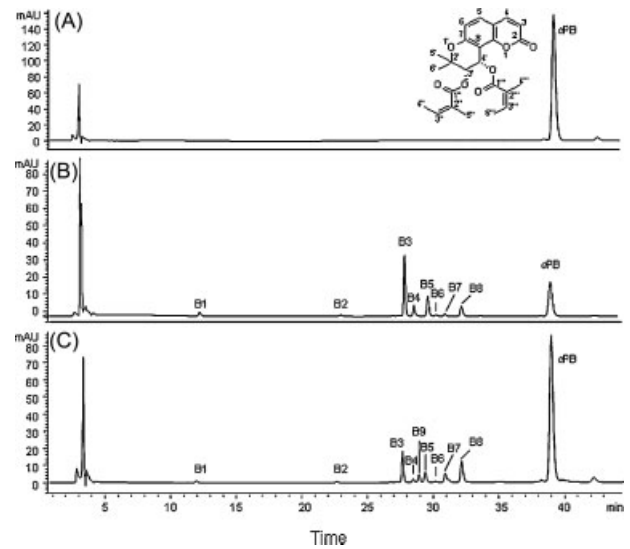

Figure 1. Representative HPLC chromatograms of incubates of *d*PB with RLMs in the absence (A) and presence (B) of a NADPH-regenerating system, or with HLMs in the presence of a NADPH-regenerating system (C), at 323 nm.

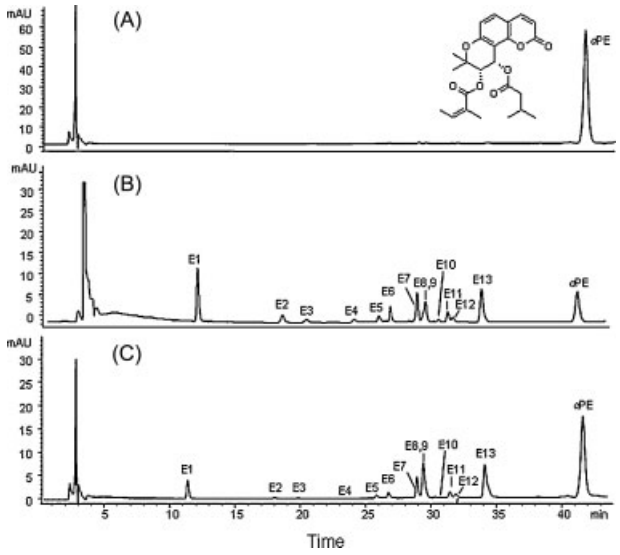

Figure 2. Representative HPLC chromatograms of incubates of *d*PE with RLMs in the absence (A) and presence (B) of a NADPH-regenerating system, or with HLMs in the presence of a NADPH-regenerating system (C), at 323 nm.

EXPERIMENTAL

Materials

*d*PB, *d*PE and (+)-praeruptorin A (*d*PA) (purity >98%) were purchased from Shanghai Traditional Chinese Medicine Research Centre (Shanghai, China). Pooled human liver microsomes (HLMs, from 15 healthy donors) were purchased from Sigma-Aldrich (St. Louis, MO, USA). A pool of rat liver microsomes (RLMs) was prepared from 30 healthy Sprague-Dawley rats (male, 250–300 g) by differential centrifugation according to a standard procedure reported previously[21] at the School of Pharmaceutical Sciences, Sun Yat-sen University (Guangzhou, China). The content of microsomal proteins was determined by Lowry's method.[22] Both HLMs and RLMs were stored at −80°C until use.

Formic acid and methanol (both HPLC grade) were purchased from Merck (Darmstadt. Germany). Ultra-pure water was obtained from a Milli-Q plus water purification system (Millipore, Bedford, MA, USA). Glucose 6-phosphate (G-6-P), glucose-6-phosphate dehydrogenase (G-6-PD) and nicotinamide adenine dinucleotide phosphate (NADP) were purchased from Sigma-Aldrich (St. Louis, MO, USA). All other chemicals were analytical grade and obtained commercially.

*d*PB and *d*PE metabolism in RLMs and HLMs

*d*PB or *d*PE (25 μM, final concentration) was incubated with 1 mg/mL of microsomal proteins in 0.1 M potassium phosphate buffer (pH 7.4) in a final incubation volume of 200 μL, at 37°C for 60 min. Reactions were initiated by addition of a NADPH-regenerating system (1 mM NADP, 1 mM glucose 6-phosphate, 1 U/mL of glucose-6-phosphate dehydrogenase) into the reaction mixtures and terminated with 200 μL of ice-cold MeOH. The sample was thoroughly mixed on a vortex mixer then centrifuged at 15 000 *g* for 10 min. An aliquot (70 μL) of the supernatant was injected for HPLC/IT-MS/MS or HPLC/TOF-MS analysis. Parallel incubations with no microsomes or no NADPH-regenerating system, and 0 min incubations, served as controls.

Preparation of (−)-*cis*-khellactone

A basic hydrolysis study of *d*PA, another main pyranocoumarin constituent from Peucedani Radix, was carried out according to a previous report[23] to aid structural identifi-

cation of B1 (one of *d*PB metabolites) or E1 (one of *d*PE metabolites) formed by liver microsomes of rats and humans. In brief, *d*PA (5 mg/mL in tetrahydrofuran) was added into 100 mL of 0.5 M KOH and the reaction mixture was stirred at 60°C for 30 min. Then 10% H_2SO_4 was added to acidify the reaction solution (pH ~6) and stirred at room temperature for 120 min before extraction with $CHCl_3$. The $CHCl_3$ layer was collected, evaporated and the residue reconstituted with methanol. The main product P1 was isolated using silica gel column chromatography (petroleum ether/ethyl acetate, 4:1 → 1:1, v/v) and identified using HPLC/MS/MS and polarimetric analysis (PerkinElmer, The Netherlands).

HPLC/MS analysis

All samples were analyzed on an Agilent series 1200 (Agilent Technologies, USA) liquid chromatography, which was equipped with a vacuum degasser, a binary pump, an autosampler and a diode-array detector (DAD) system, and operated with Agilent ChemStation B 3.0 software. The analytical column was an ODS reversed-phase C_{18} column (250 mm × 4.6 mm i.d., particle size 5 μm, Agilent, USA). The column temperature was maintained at 35°C. The mobile phase consisted of 0.1% aqueous formic acid (A) and methanol (B). Samples were analyzed using a gradient elution as follows: 0–4 min, 25%–50% B; 4–16 min, 50%–53% B; 16–17 min, 53%–56% B; 17–20 min, 56% B; 20–23 min, 56%–69% B; 23–40 min, 69%–76% B; 40–41 min, 76%–100% B; 41–44min, 100% B. The flow rate was set at 1.0 mL/min and the injection volume was 70 μL. The sample chamber temperature was set at 4°C. The respective parent compound and its metabolites were monitored at 323 nm.

Ion trap tandem mass spectrometry analysis (IT-MS/MS) was performed on an Agilent MSD Ion Trap system (Palo Alto, CA, USA) coupled to an electrospray ionization (ESI) interface. A quarter of the column eluent was directly introduced into the ESI interface through a PEEK tubing (0.13 mm i.d.). Nitrogen was used as both the nebulizing gas at 45 psi and the drying gas at a flow rate of 8 L/min at a temperature of 350°C. The mass spectrometer was operated in positive ion mode over a mass range of 100–500 *m/z*. Helium was used as the collision gas for the tandem mass spectrometry experiments. Fragmentation was induced with the resonant excitation amplitude of 0.6 V, followed by an isolation of the precursor ion over a selected mass window of 1 Da. Data acquisition was performed using Agilent ChemStation software (Agilent Technologies, MA, USA).

High-resolution mass spectrometry (HR-MS) analysis was performed on an Agilent 6210 TOF mass spectrometer (Agilent Technologies, USA) that operated in positive ESI mode. The parameters of the ion source were set as capillary voltage of 4500 V and drying gas (N_2) pressure of 20 psi. MS conditions were as follows: mass range, 100–1000 *m/z*; fragmentor voltage, 250 V; skimmer voltage, 60 V. The instrument performed automatic runs by introducing a constant flow of calibrating solution containing the ESI-TOF tuning reference solution and API-TOF reference mass solution (Agilent Technologies, USA).

RESULTS AND DISCUSSION

HPLC/MS/MS and TOF-MS analysis of *d*PB, *d*PE and (−)-*cis*-khellactone

Under the developed analytical conditions, *d*PB and *d*PE were eluted at 38.0 min and 42.6 min, respectively, and most of metabolites and their respective parent compounds obtained baseline separation (Figs. 1–4). The accurate mass, estimated elemental composition, error in terms of ppm and sequential mass (MS^1 and MS^2) data of the parent compounds are listed in Tables 1 and 2 and provided additional information for identification of their metabolites produced in liver microsomes of rats and humans.

The MS^1 spectrum of *d*PB exhibited adduct ions at *m/z* 444 ($[M+NH_4]^+$) and *m/z* 449 ($[M+Na]^+$), corresponding to the molecular weight of 426 Da for *d*PB. And TOF-MS analysis revealed a sodiated adduct ion at *m/z* 449.1567 and provided an elemental composition of $C_{24}H_{26}O_7$. MS^2 of the sodiated adduct ion at *m/z* 449 ($[M+Na]^+$) revealed two major product ions at *m/z* 349 and *m/z* 327 resulting from the loss of the C_4H_7COOH and C_4H_7COONa moieties, respectively, from the C-3′ or C-4′ position (Table 1, Fig. 5). The characteristic ion at *m/z* 245 corresponds to the cleavage of an angeloyl group from *m/z* 327. Moreover, the characteristic ion at *m/z* 227 corresponds to loss of a water molecule and a C_3H_6 molecule from the khellactone skeleton or an angelic acid molecule (C_4H_7COOH) from *m/z* 327.

*d*PE was eluted at 42.6 min. Its mass spectra revealed a fragmentation pattern similar to that of *d*PB: adduct ions at *m/z* 446 ($[M+NH_4]^+$) and *m/z* 451 ($[M+Na]^+$) observed in the MS^1 spectrum correspond to a molecular weight of 428 Da for *d*PE. Accurate mass data showed the adduct ions at *m/z* 446.2188 and *m/z* 451.1737 and gave a molecular formula of $C_{24}H_{28}O_7$. The MS^2 spectrum of the sodiated adduct ion exhibited product ions at *m/z* 349 and *m/z* 327, which indicate the loss of C_4H_9COOH and C_4H_9COONa from the C-4′ position, respectively. The presence of the characteristic ions at *m/z* 245 and *m/z* 227 suggests further loss of a C_4H_6CO moiety and a C_4H_7COOH molecule at the C-3′ position, respectively (Table 2, Fig. 6).

The sequential mass spectrometric analysis of *d*PB and *d*PE revealed common characteristic product ions at *m/z* 349, *m/z* 327, *m/z* 245 and *m/z* 227 in MS^2 spectra (Tables 1 and 2), supporting removal of two RCOOH units substituted at the C-3′ and C-4′ positions, respectively. In an MS^n study of pyranocoumarin constituents from Peucedani Radix, the authors proposed that the fragmentation of an angular-type pyranocoumarin usually initiates from the 4′ position when the two substituents connected to the C-3′ and C-4′ positions were different.[24] In the present study, the mass fragmentation preference of *d*PE agrees well with the speculation of Tao *et al.*,[24] whereas the mass data obtained for *d*PB could not definitely support such mass fragmentation preference due to the identical groups substituted at the C-3′ and C-4′ positions of this compound.

When *d*PA, an angular-type pyranocoumarin which has an angeloyl moiety and an acetyl moiety substituted at the C-3′ and C-4′ positions, respectively, was treated with KOH, three products were yielded from the basic hydrolysis (Fig. 7). The product P1 was eluted at 11.9 min and exhibited adduct ions at *m/z* 285 ($[M+Na]^+$) and *m/z* 301 ($[M+K]^+$) and

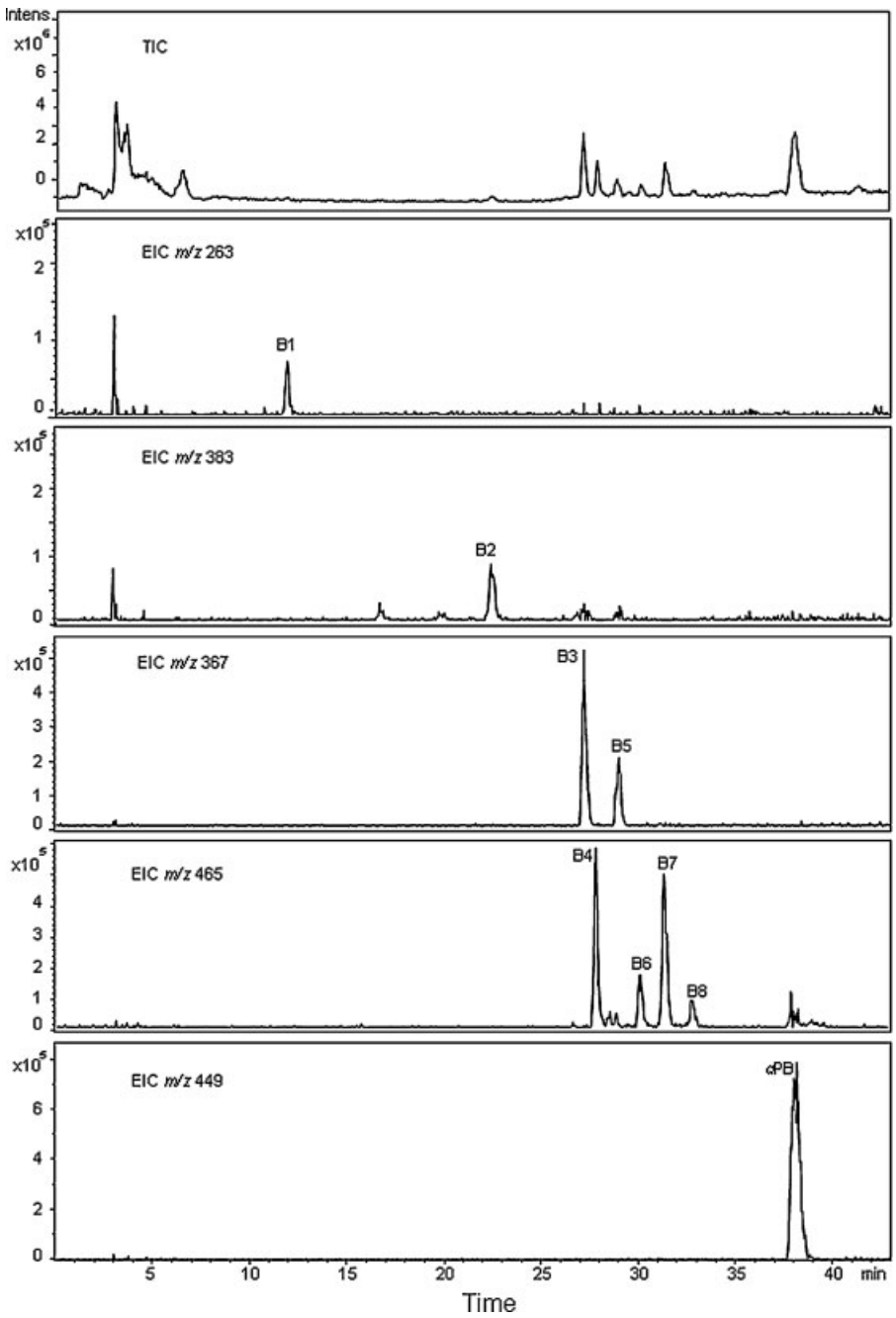

Figure 3. Representative total ion current chromatogram and extracted ion chromatograms of *d*PB and its metabolites produced following incubation with RLMs in the presence of a NADPH-regenerating system.

the protonated ion at *m*/*z* 263 ($[M+H]^+$), indicating a molecular weight of 262 Da. Accurate mass analysis indicated that the elemental composition of P1 is $C_{14}H_{14}O_5$. MS^2 of the protonated ion resulted in two product ions: *m*/*z* 245 corresponding to loss of a water molecule and *m*/*z* 203 for loss of a water molecule plus a C_3H_6 molecule. These mass spectra, the retention time and UV spectrum of P1 were identical with those of (−)-*cis*-khellactone, which was prepared from *d*PA by the same method and unambiguously identified on the basis of HPLC/MS/MS and NMR analyses by Wu and co-workers.[23] Thus, P1 produced in the present study was assigned as (−)-*cis*-khellactone, which was derived from removal of both angeloyl and acetyl moieties from the C-3′ and C-4′ positions of *d*PA.

In vitro metabolism of *d*PB and *d*PE in liver microsomes of rats and humans

The representative HPLC-UV chromatograms, total ion current (TIC) chromatograms and extracted ion current (EIC) chromatograms of samples obtained from reactions of *d*PB and *d*PE with liver microsomes are shown in Figs. 1–4. The MS^1 and MS^2 spectra of *d*PB and *d*PE metabolites are shown in Figs. 5 and 6 and chromatographic and mass

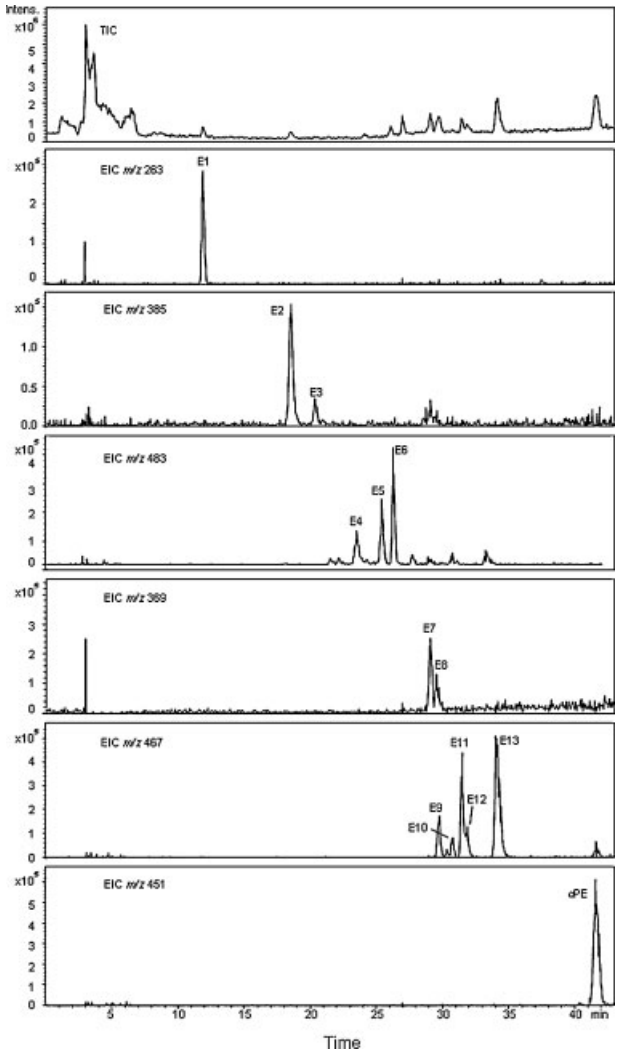

Figure 4. Representative total ion current chromatogram and extracted ion chromatograms of *d*PE and its metabolites produced following incubation with RLMs in the presence of a NADPH-regenerating system.

spectrometric data are summarized in Tables 1 and 2 and compared with those of the parent compounds. Metabolites of *d*PB and *d*PE showed similar mass fragmentation profiles to their respective parent compound.

The incubation of *d*PB with rat liver microsomal proteins resulted in eight metabolites (B1–8), while one additional metabolite (B9) that eluted between B4 and B5 was observed in HLMs (Fig. 1). A total of 13 metabolites (E1–13) of *d*PE were generated in liver microsomes of both species (Fig. 2). All the metabolites were eluted earlier than the respective parent compound and formed in a NADPH-dependent manner, indicating that the metabolites are more polar than their respective parent compound and their formations are catalyzed by cytochrome P450 isozyme(s).

The metabolites of *d*PB formed in rat and human liver microsomes

The eight metabolites (B1–B8) of *d*PB detected in RLMs were identical with those found in HLMs as judged by their retention times, UV spectra, mass spectra and accurate mass data (Figs. 1 and 3, Table 1), indicating that *d*PB undergoes similar biotransformations in liver microsomes of both species.

Similar to the MS^1 spectrum of *d*PB, sodiated adduct ions ($[M+Na]^+$) at significant intensity were observed for B2–B8; thus the sodiated adduct ions were used to produce MS^2 spectra of these metabolites (Fig. 3, Table 1). In contrast, a strong signal of the protonated ion ($[M+H]^+$) was observed in MS^1 of B1 and applied for MS^2 scan of this metabolite. In addition, the characteristic ions at *m/z* 245, *m/z* 227 and *m/z* 203 were commonly observed in MS^2 spectra of most metabolites. The identity of B9, the metabolite only found in HLMs, could not be elucidated based on the available mass data (data not shown).

B1 was eluted at 11.9 min. Its MS^1 spectrum showed the protonated ion at *m/z* 263 ($[M+H]^+$), sodiated adduct ion at *m/z* 285 ($[M+Na]^+$) and potassiated adduct ion at *m/z* 301 ($[M+K]^+$), suggesting that the molecular weight of B1 is 262 Da. TOF-MS also provided the accurate mass data at *m/z* 263.0915 ($[M+H]^+$), *m/z* 285.0731 ($[M+Na]^+$) and *m/z* 301.0468 ($[M+K]^+$), respectively, and gave a formula of $C_{14}H_{14}O_5$, which corresponds to removal of both angeloyl moieties from the C-3′ and C-4′ positions of *d*PB (Fig. 5). The characteristic ions at *m/z* 245 and *m/z* 203 present in the MS^2 spectrum correspond to the loss of a water molecule, a water molecule together with a C_3H_6 molecule, respectively, from the protonated ion. Thus, B1 should have resulted from hydrolytic removal of both C-3′ and C-4′ angeloyl groups from *d*PB by liver microsomal proteins. Furthermore, B1 showed identical retention times, UV and mass spectra, and accurate mass data to those of (−)-*cis*-khellactone (P1), the product yielded from basic hydrolysis of *d*PA (Fig. 7). Finally, B1 was identified as (−)-*cis*-khellactone.

B2 was observed at a retention time of 22.2 min and exhibited adduct ions at *m/z* 383 ($[M+Na]^+$) and *m/z* 399 ($[M+K]^+$), suggesting a molecular weight of 360 Da, 66 Da lower than its parent compound (Figs. 1 and 5). Accurate mass data supported a molecular formula of $C_{19}H_{20}O_7$ (Table 1). Further, the MS^2 of the sodiated ion at *m/z* 383 revealed a major product ion at *m/z* 267, which was 116 mass units less than the precursor ion and corresponds to loss of a mono-oxidized angelic acid molecule. Thus B2 was speculated as a product formed from cleavage of one angeloyl group concomitant with mono-oxidation on the other angeloyl group of *d*PB (Fig. 8). The oxidation on the side chain could be hydroxylation at the C-3‴, 4‴, or 5‴ position, or cyclo-oxidation at the double bond.

B3 and B5 showed similar MS^1 and MS^2 spectra yet different retention times (B3, 27.1 min; B5, 28.8 min), suggesting that these two metabolites are isomers. The MS^1 spectra showed adduct ions at *m/z* 362 ($[M+NH_4]^+$) and *m/z* 367 ($[M+Na]^+$), indicating the molecular weights of B3 and B5 are 344 Da and 82 Da lower than *d*PB and 16 Da lower than B2. TOF-MS analysis revealed identical sodiated adduct ions at *m/z* 367.1154 and provided the same molecular formula of $C_{19}H_{20}O_6$ for both metabolites. In the MS^2 spectrum of the sodiated adduct ion, the presence of the predominant product ion at *m/z* 267 indicates the loss of one C_4H_7COOH molecule. Thus B3 and B5 might be positional isomers with one being 3′-*O*-angeloyl khellactone and the other 4′-*O*-angeloyl khellactone, or stereoisomers of 3′-*O*-angeloyl

Table 1. Chromatographic and mass spectrometric data of *d*PB and its metabolites formed in liver microsomes of rats and humans

Compound	Rt (min)	MS^1	Measured mass	Elemental composition	Error (ppm)	Molecular formula	MS^2
*d*PB	38.0	$444[M+NH_4]^+$ $449[M+Na]^+$	449.1567	$C_{24}H_{26}O_7Na$	0.97	$C_{24}H_{26}O_7$	$349[M+Na-C_4H_7COOH]^+$ $327[M+H-C_4H_7COOH]^+$ $245[327-C_4H_7COOH]^+$, 227
B1	11.9	$263[M+H]^+$ $285[M+Na]^+$ $301[M+K]^+$	263.0915 285.0731 301.0468	$C_{14}H_{15}O_5$ $C_{14}H_{14}O_5Na$ $C_{14}H_{14}O_5K$	−0.24 0.95 1.82	$C_{14}H_{14}O_5$	$245[M+H-H_2O]^+$, $203[245-C_3H_6]^+$
B2	22.2	$383[M+Na]^+$ $399[M+K]^+$	383.1106 399.0851	$C_{19}H_{20}O_7Na$ $C_{19}H_{20}O_7K$	−1.23 −2.82	$C_{19}H_{20}O_7$	$267[M+Na-HOC_4H_6COOH]^+$
B3	27.1	$362[M+NH_4]^+$ $367[M+Na]^+$	367.1153	$C_{19}H_{20}O_6Na$	−0.24	$C_{19}H_{20}O_6$	$267[M+Na-C_4H_7COOH]^+$
B4	27.8	$460[M+NH_4]^+$ $465[M+Na]^+$	465.1524	$C_{24}H_{26}O_8Na$	−0.54	$C_{24}H_{26}O_8$	$365[M+Na-C_4H_7COOH]^+$ $245[365-HOC_4H_6COONa]^+$, 227, 203
B5	28.8	$345[M+H]^+$ $362[M+NH_4]^+$ $367[M+Na]^+$	345.1336 367.1154	$C_{19}H_{21}O_6$ $C_{19}H_{20}O_6Na$	−0.98 −0.47	$C_{19}H_{20}O_6$	$267[M+Na-C_4H_7COOH]^+$
B6	30.0	$460[M+NH_4]^+$ $465[M+Na]^+$	465.1522	$C_{24}H_{26}O_8Na$	−0.56	$C_{24}H_{26}O_8$	$365[M+Na-C_4H_7COOH]^+$ $245[365-HOC_4H_6COONa]^+$, 227, 203
B7	31.3	$460[M+NH_4]^+$ $465[M+Na]^+$	465.1526	$C_{24}H_{26}O_8Na$	−1.28	$C_{24}H_{26}O_8$	$365[M+Na-C_4H_7COOH]^+$ $245[365-HOC_4H_6COONa]^+$, 227, 203
B8	33.8	$460[M+NH_4]^+$ $465[M+Na]^+$	465.1521	$C_{24}H_{26}O_8Na$	−0.25	$C_{24}H_{26}O_8$	$349[M+Na-HOC_4H_6COOH]^+$ $327[M+H-HOC_4H_6COOH]^+$, 227

khellactone with one as the *R*-isomer and the other as the *S*-isomer.

B4, B6, B7 and B8 were eluted at 27.8 min, 30.0 min, 31.3 min and 33.8 min, respectively, yet showed the same characteristic ions, including *m/z* 465 ($[M+Na]^+$), *m/z* 460 ($[M+NH4]^+$), *m/z* 343 ($[M-C_4H_7COOH]^+$) and *m/z* 245 ($[M-2C_4H_7COOH]^+$) in their MS spectra, thus B4, B6, B7 and B8 should be four isomers with molecular weights of 442 Da, 16 Da higher than *d*PB, indicating that these four metabolites are all mono-oxidized products of *d*PB. TOF-MS also resulted in identical sodiated adduct ions and the same elemental composition of $C_{24}H_{26}O_8$ for the four metabolites. Interestingly, MS^2 spectra of the sodiated adduct ion revealed distinct fragmentation profiles: The characteristic ion at *m/z* 365 was found with B4, B6 and B7 and supported the loss of one C_4H_7COOH molecule while the fragment ion at *m/z* 349 in B8 corresponds to the loss of the oxidized angeloyl group (Table 1, Fig. 5). This distinct fragmentation profile might be a result of mono-oxidation occurring at a different side chain. The mono-oxidation might occur via direct hydroxylation of C-4‴ or C-5‴, or via cyclooxidation of the double bond of the side chain substituted at either the C-3′ or C-4′ position.

The metabolites of *d*PE formed by rat and human liver microsomes

The incubation of *d*PE with RLMs and HLMs yielded the same 13 metabolites as judged by identical retention times, UV and mass spectra and accurate mass data (Figs. 2 and 4, Table 2), indicating that *d*PE undergoes similar biotransformations in liver microsomes of both species.

Chromatographic and mass spectrometric data of *d*PE and its metabolites E1–E13 are summarized in Table 2. The mass spectra of *d*PE and metabolites E4–6, three metabolites formed via di-oxidation that were absent with *d*PB, are shown in Fig. 6. Similar to that of *d*PB, the MS^1 spectra of most of its metabolites exhibited intense sodiated adduct ions, which were used as precursor ions for MS^2 analysis, yet E1 showed the protonated ion as base peak, which was the precursor ion of MS^2 analysis. In addition, a potassium adduct ion appeared in the mass spectra of *d*PE and all its metabolites. Again, the characteristic ions at *m/z* 245 and *m/z* 227 were commonly found in MS^2 spectra of most *d*PE metabolites, indicating that these metabolites follow a similar fragmentation pathway to *d*PB metabolites.

E1 was eluted at 11.9 min and showed identical retention time, MS^1 and MS^2 spectra, and accurate mass data with those of B1 formed from *d*PB and (−)-*cis*-khellactone produced from *d*PA, thus E1 was also identified as (−)-*cis*-khellactone, which was formed from hydrolysis of both the angeloyl group and the isovaleryl group from the C-3′ and C-4′ positions of *d*PE, respectively (Table 2, Fig. 9).

E2 and E3 were observed at the retention times of 18.2 min and 20.1 min, respectively, and exhibited similar characteristic ions at *m/z* 385 ($[M+Na]^+$) and *m/z* 401 ($[M+K]^+$) in their MS^1 spectra, indicating that E2 and E3 are isomers with the molecular weight of 362 Da, which was 66 Da lower than *d*PE (molecular weight: 428 Da). TOF-MS also revealed identical elemental compositions and molecular formulas of $C_{19}H_{22}O_7$ for both metabolites. In addition, the product ions at *m/z* 245 in MS^1 spectra and *m/z* 267 in MS^2 of the sodiated adduct ion correspond to the loss of HOC_4H_8COONa and HOC_4H_8-COOH molecules from the precursor ion at *m/z* 385,

Rapid Communications in Mass Spectrometry

Table 2. Chromatographic and mass spectrometric data of *d*PE and its metabolites formed in liver microsomes of rats and humans

Compound	Rt (min)	MS^1	Measured Mass	Elemental composition	Error (ppm)	Molecular formula	MS^2
*d*PE	42.6	446[M+NH_4]$^+$	446.2188	$C_{24}H_{28}O_8NH_4$	−1.34	$C_{24}H_{28}O_8$	349[M+Na–C_4H_9COOH]$^+$
		451[M+Na]$^+$	451.1737	$C_{24}H_{28}O_8Na$	−2.22		327[M+H–C_4H_9COOH]$^+$
		467[M+K]$^+$					
E1	11.9	263[M+H]$^+$	263.0920	$C_{14}H_{15}O_5$	−2.23	$C_{14}H_{14}O_5$	245[M+H–H_2O]$^+$
		285[M+Na]$^+$	285.0737	$C_{14}H_{14}O_5Na$	−1.54		
		301[M+K]$^+$	301.0474	$C_{14}H_{14}O_5K$	0.55		
E2	18.2	385[M+Na]$^+$	385.1266	$C_{19}H_{22}O_7Na$	−2.26	$C_{19}H_{22}O_7$	267[M+Na–HOC_4H_8COOH]$^+$
		401[M+K]$^+$	401.1010	$C_{19}H_{22}O_7K$	−3.61		245[M+H–HOC_4H_8COOH]$^+$
E3	20.1	385[M+Na]$^+$	385.1258	$C_{19}H_{22}O_7Na$	−2.85	$C_{19}H_{22}O_7$	267[M+Na–HOC_4H_8COOH]$^+$
		401[M+K]$^+$	401.1004	$C_{19}H_{22}O_7K$	−2.03		245[M+H–HOC_4H_8COOH]$^+$
E4	24.0	483[M+Na]$^+$	483.1625	$C_{24}H_{28}O_9Na$	0.13	$C_{24}H_{28}O_9$	365[M+Na–HOC_4H_8COOH]$^+$
		499[M+K]$^+$	499.1363	$C_{24}H_{28}O_9K$	0.45		343[M+H–HOC_4H_8COOH]$^+$
							245[365–HOC_4H_6CONa]$^+$, 227
E5	25.9	483[M+Na]$^+$	483.1646	$C_{24}H_{28}O_9Na$	−4.48	$C_{24}H_{28}O_9$	365[M+Na–HOC_4H_8COOH]$^+$
		499[M+K]$^+$	499.1378	$C_{24}H_{28}O_9K$	−2.78		343[M+H–HOC_4H_8COOH]$^+$
							245[365–HOC_4H_6CONa]$^+$, 227
E6	26.9	483[M+Na]$^+$	483.1634	$C_{24}H_{28}O_9Na$	−1.81	$C_{24}H_{28}O_9$	365[M+Na–HOC_4H_8COOH]$^+$
		499[M+K]$^+$	499.1364	$C_{24}H_{28}O_9K$	0.23		343[M+H–HOC_4H_8COOH]$^+$
							245[365–HOC_4H_6CONa]$^+$, 227
E7	29.0	364[M+NH_4]$^+$				$C_{19}H_{22}O_6$	267[M+Na–C_4H_9COOH]$^+$
		369[M+Na]$^+$	369.1309	$C_{19}H_{22}O_6Na$	−0.21		245[M+H–C_4H_9COOH]$^+$
		385[M+K]$^+$	385.1053	$C_{19}H_{22}O_6K$	−1.53		
E8	29.5	364[M+NH_4]$^+$				$C_{19}H_{22}O_6$	267[M+Na–C_4H_9COOH]$^+$
		369[M+Na]$^+$	369.1310	$C_{19}H_{22}O_6Na$	−0.41		245[M+H–C_4H_9COOH]$^+$
		385[M+K]$^+$	385.1055	$C_{19}H_{22}O_6K$	−2.10		
E9	29.5	462[M+NH_4]$^+$	462.2128	$C_{24}H_{28}O_8NH_4$	−1.34	$C_{24}H_{28}O_8$	365[M+Na–C_4H_9COOH]$^+$
		467[M+Na]$^+$	467.1617	$C_{24}H_{28}O_8Na$	1.22		343[M+H–C_4H_9COOH]$^+$
		483[M+K]$^+$	483.1415	$C_{24}H_{28}O_8K$	0.07		
E10	30.7	462[M+NH_4]$^+$				$C_{24}H_{28}O_8$	365[M+Na–C_4H_9COOH]$^+$
		467[M+Na]$^+$	467.1676	$C_{24}H_{28}O_8Na$	0.15		343[M+H–C_4H_9COOH]$^+$
		483[M+K]$^+$	483.1416	$C_{24}H_{28}O_8K$	−0.01		
E11	31.3	467[M+Na]$^+$	467.1784	$C_{24}H_{28}O_8Na$	−1.32	$C_{24}H_{28}O_8$	349[M+Na–HOC_4H_8COOH]$^+$
		483[M+K]$^+$	483.1427	$C_{24}H_{28}O_8K$	−2.56		327[M+H–HOC_4H_8COOH]$^+$
E12	31.7	462[M+NH_4]$^+$				$C_{24}H_{28}O_8$	365[M+Na–C_4H_9COOH]$^+$
		467[M+Na]$^+$	467.1684	$C_{24}H_{28}O_8Na$	−1.63		343[M+H–C_4H_9COOH]$^+$
		483[M+K]$^+$	483.1426	$C_{24}H_{28}O_8K$	−2.24		
E13	34.0	462[M+NH_4]$^+$	462.2137	$C_{24}H_{28}O_8NH_4$	−3.35	$C_{24}H_{28}O_8$	365[M+Na–C_4H_9COOH]$^+$
		467[M+Na]$^+$	467.1683	$C_{24}H_{28}O_8Na$	−1.40		343[M+H–C_4H_9COOH]$^+$
		483[M+K]$^+$	483.1422	$C_{24}H_{28}O_8K$	−1.53		

supporting occurrence of hydroxylation on the isovaleryl group substituted at the C-4′ position. Thus, E2 and E3 should be positional isomers that are formed from a combination of removal of the angeloyl group via hydrolysis and hydroxylation on the isovaleryl substituent of *d*PE (Table 1 and Fig. 9). The hydroxyl group could be introduced at the C-2‴, C-3‴, C-4‴ or C-5‴ position of the isovaleryl group.

E4, E5 and E6 showed similar MS^1 and MS^2 spectra yet different retention times (E4, 24.0 min; E5, 25.9 min; E6, 26.9 min), suggesting that these three metabolites are isomers. In MS^1 spectra, the adduct ions at *m/z* 483 ([M+Na]$^+$) and *m/z* 499 ([M+K]$^+$) indicated the molecular weight of 460 Da, 32 Da higher than *d*PE, suggesting the occurrence of di-oxidation, which was supported by molecular formulas of $C_{24}H_{28}O_9$ as revealed by TOF-MS analysis. The characteristic ion at *m/z* 365 in MS^2 spectra corresponds to the loss of a mono-hydroxylated C_4H_9COOH molecule, indicating that there is one hydroxyl substituent on the isovaleryl group and the other oxygen atom should be introduced into the C-3′ angeloyl moiety. Therefore, E3, E4 and E5 were tentatively identified as positional isomers formed from di-oxidation of *d*PE with one oxygen atom introduced into the isovaleryl group and the other into the angeloyl group, respectively (Table 1 and Fig. 9).

E7 and E8 showed similar MS^1 and MS^2 spectra and accurate mass data yet different retention times (E7, 29.0 min; E8, 29.5 min). Their MS^1 spectra showed adduct ions at *m/z* 364 ([M+NH_4]$^+$), *m/z* 369 ([M+Na]$^+$) and *m/z* 385 ([M+K]$^+$), indicating the molecular weight of 346 Da, 82 Da lower than *d*PE and 16 Da lower than the mono-hydroxylated metabolites E2 and E3. The molecular formulas are $C_{19}H_{22}O_6$ as measured by TOF-MS. The MS^2 of the sodiated adduct ion at *m/z* 369 of the two compounds revealed a predominant product ion at *m/z* 267, 102 Da less than the precursor ion, corresponding to the loss of the C-4′ isovaleryl moiety (C_4H_9COOH). Therefore, the identities of E7 and E8 were

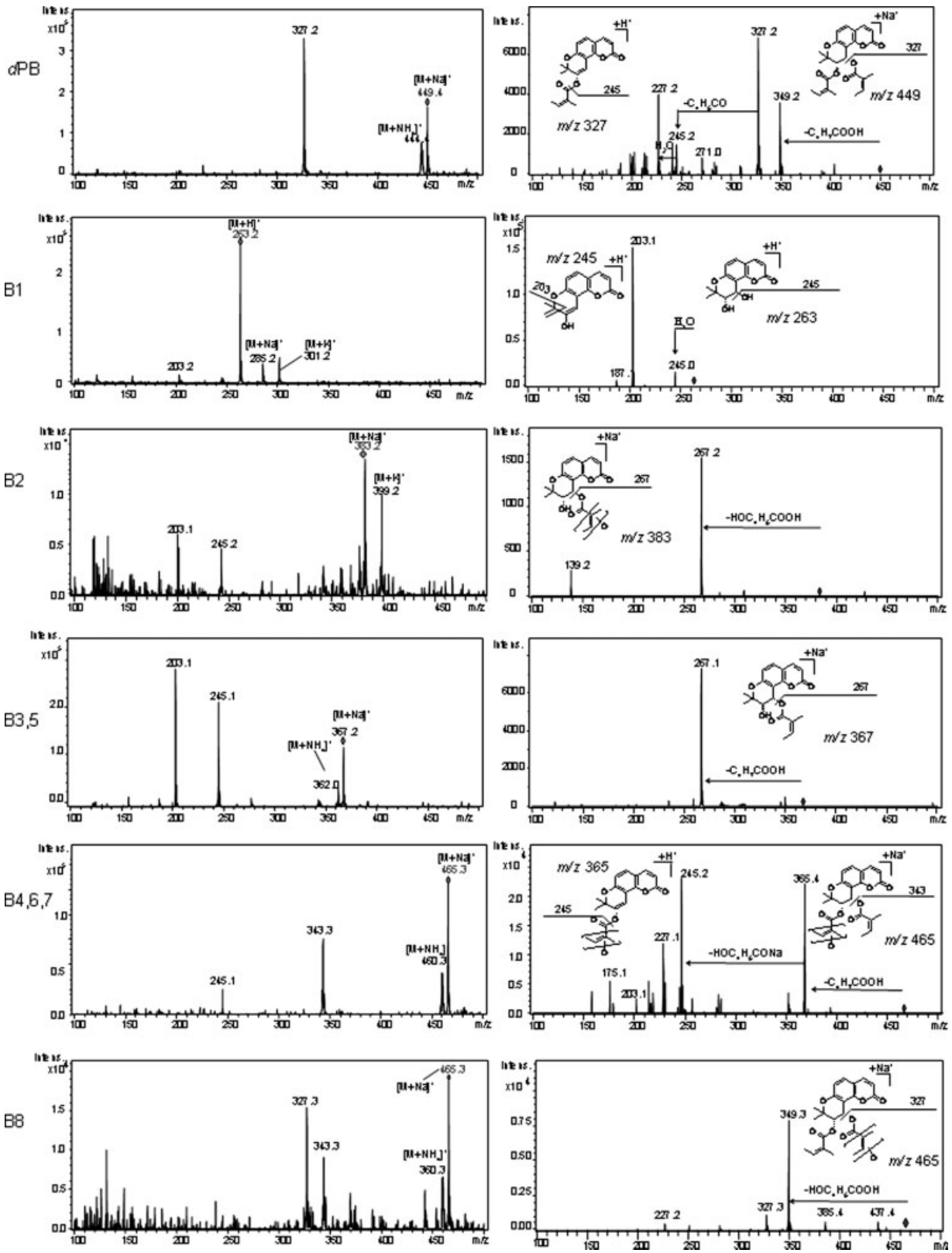

Figure 5. MS^1 (left) and MS^2 (right) spectra of *d*PB and its metabolites B1–B8 formed in liver microsomes of rats and humans.

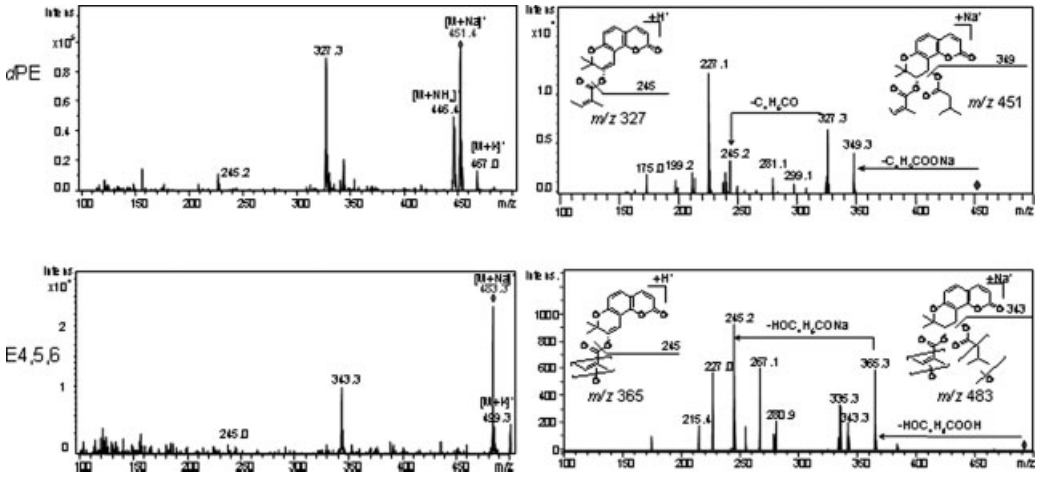

Figure 6. MS^1 (left) and MS^2 (right) spectra of *d*PE and its metabolites E4–E6 formed in liver microsomes of rats and humans.

tentatively assigned as stereoisomers of 4′-*O*-isovaleryl khellactone (Fig. 9) with one as the *R*-isomer and the other the *S*-isomer.

E9, E10, E11, E12 and E13 were the last five metabolites eluted between 29–34 min sequentially. The MS^1 spectra of all five metabolites exhibited a sodiated adduct ion at *m/z* 467 ($[M+Na]^+$), indicating their molecular weight of 444 Da, 16 Da higher than *d*PE. TOF-MS analysis indicated the same molecular formula of $C_{24}H_{28}O_8$ for all five metabolites. Thus, these five metabolites might be mono-oxidized products of *d*PE. Interestingly, MS^2 of the sodiated ions of the five metabolites resulted in distinct product ions: the major product ion at *m/z* 365 ($[M+Na–C_4H_9COOH]^+$) for E9, E10, E12 and E13, yet the major product ions at *m/z* 349 ($[M+Na–HOC_4H_8COOH]^+$) and *m/z* 327 ($[M+H–HOC_4H_8COOH]^+$) for E11. These findings suggested that the mono-oxidation occurs on the angeloyl group of E9, E10, E12 and E13 but on the isovaleryl group of E11 (Table 1, Fig. 9). Since the C-3′ angeloyl moiety has four potential sites for mono-oxidation, including hydroxylation at C-3″, C-4″ and C-5″, and cyclooxidation of the double bond between C-2″ and C-3″, it is reasonable to deduce that three of the four metabolites E9, E10, E12 and E13 were formed via hydroxylation on the angeloyl group and one of them was generated via cyclo-oxidation. In the case of E11, there are also four potential sites (C-2‴, C-3‴, C-4‴ and C-5‴) of hydroxylation on the isovaleryl group but only one metabolite M11 was observed, thus the exact position of mono-oxidation could not be definitely assigned.

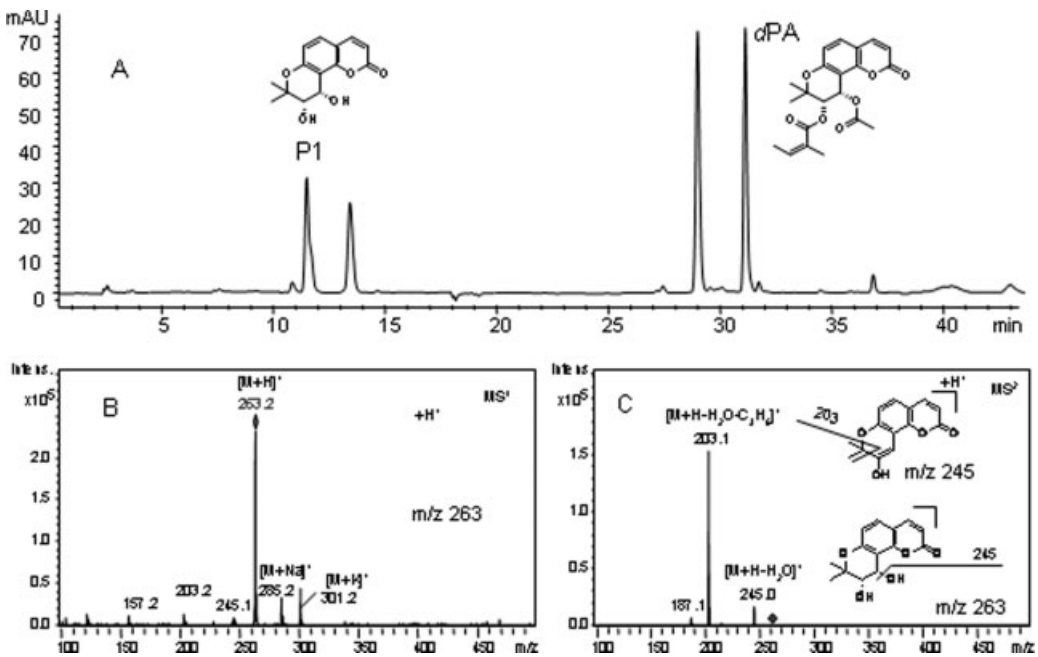

Figure 7. The HPLC chromatogram of the sample from basic hydrolysis of *d*PA (A) and MS^1 (B) and MS^2 (C) spectra of the main product (−)-*cis*-khellactone (P1).

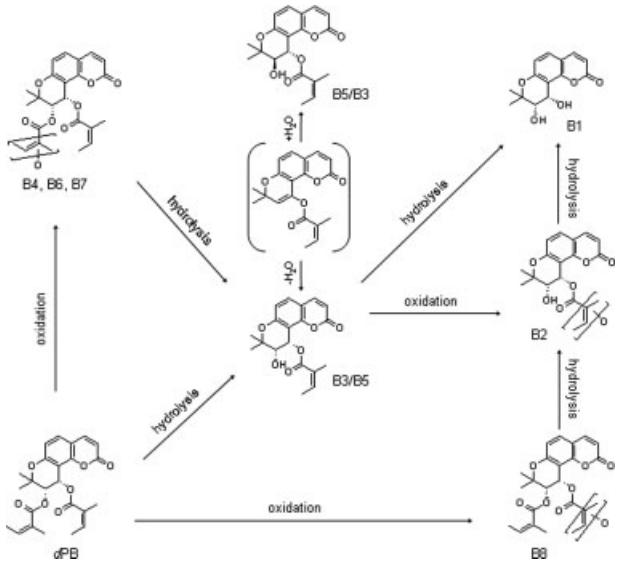

Figure 8. Proposed metabolic pathways of *d*PB in liver microsomes of rats and humans. The intermediate is shown in brackets.

Metabolic difference between *d*PB and *d*PE in rat and human liver microsomes

In general, *d*PE was eliminated slightly faster than *d*PB in liver microsomes of both species (percentage of remaining: *d*PE, 15% (rat) and 41% (human); *d*PB, 25% (rat) and 51% (human)).

In the present study, the mass fragmentation profiles of *d*PE, of which the C-3′ and C-4′ positions are substituted with different groups (angeloyl and isovaleryl group, respectively), and its metabolites, revealed a preference of cleavage of the C-3′ angeloyl substituent. This finding agrees well with the ESI-MS^n profiles of pyranocoumarins from Peucedani Radix reported by Tao *et al*.[24] Thus, the metabolic pathway of *d*PE was easily proposed (Fig. 9). *d*PB has two angeloyl moieties substituted at the C-3′ and C-4′ positions. Although hydrolysis and oxidation could be concluded as the two predominant pathways of *d*PB metabolism by liver microsomal proteins of rats and humans, the exact site of hydrolysis was not readily speculated based on the mass fragmentation patterns of *d*PB and its metabolites. Since *d*PB metabolites (except for B1 which has two adjacent hydroxyl groups) possess different substituents at the C-3′ and C-4′ positions and exhibit similar mass fragmentation patterns to those of *d*PE, *d*PE metabolites and the angular-type pyranocoumarin constituents from Peucedani herb,[24,25] the mass fragmentation preference at the C-4′ position might also be applicable to B2–B8. Thus the structures of these metabolites and the metabolic pathway of *d*PB in RLMs and HLMs were proposed (Fig. 8).

As shown in Figs. 8 and 9, oxidation and hydrolysis were the two predominant pathways of *d*PB and *d*PE metabolism in rat and human liver microsomal proteins and occurred only on the aliphatic chain. Although oxidation could be initiated on either the C-3′ or C-4′ substituent, hydrolysis was only initiated at the C-3′ substituent. Moreover, di-oxidation was observed with *d*PE yet was absent with *d*PB. In a recent report on the metabolic study of 3′,4′-di-*O*-(−)-camphanoyl-(+)-*cis*-khellactone derivatives (DCKs) in HLMs, a rapid mono-oxidation of these DCKs on the lipophilic camphanoyl moieties substituted at the C-3′ or C-4′ positions was also observed.[26] In contrast to hydrolysis as one of the predominant pathways of *d*PB and *d*PE metabolisms in both RLMs and HLMs that were found in the present study, no hydrolysis of either camphanoyl ester moiety of DCKs was observed and the authors speculated a steric hindrance of the bulky camphanoyl structure as the cause. Taken together, these findings indicate that the C-3′ and C-4′ substituents on khellactone are determinant factors for the metabolic properties (metabolic pathway and extent of metabolism) of these angular-type pyranocoumarins.

There were two isomers (B3 and B5, E7 and E8) formed from hydrolytic removal of the C-3′ ester group of *d*PB and *d*PE, respectively (Figs. 8 and 9). The mass profiles of E7 and E8 indicated two stereoisomers with one as the *R*-isomer and the other as the *S*-isomer. Generally, direct hydrolysis of the C-3′ moiety should result in the *R*-isomer without changing the configuration. The formation of the *S*-isomer was proposed as follows: The *R*-isomer loses a water molecule from the exposed hydroxyl group at the C-4′ position and the adjacent C-4′ ester group to form a double bond between C-3′ and C-4′. This newly formed alkene functional group might be unstable and undergoes hydration in the aqueous media to give both *R*- and *S*-isomers. The formation of two stereoisomers from removal of the C-3′ ester group has been definitely supported by NMR analysis of the metabolites of *l*-praeruptorin A, another pyranocoumarin isolated from Peucedani Radix, and seems to be a common metabolic pathway of angular-type pyranocoumarins in liver microsomal proteins (unpublished data from our research group). Accordingly, the metabolic pathway of *d*PB was proposed, and B3 and B5 were tentatively assigned as stereoisomers of 3′-*O*-angeloyl khellactone. However, further hydrolysis of the C-4′ ester group only resulted in one metabolite, (−)-*cis*-khellactone, of which the configuration is the same as the parent compounds. This might be a result of a subsequent stereoselective hydrolysis of the isomers catalyzed by NADPH-independent carboxylesterase(s).[27–29]

Furthermore, slight species difference in *d*PB and *d*PE metabolisms was evidenced by the metabolites formed and the relative ratio of each metabolite. RLMs used in the present study showed higher capability in catalyzing both *d*PB and *d*PE metabolisms (percentages of the parent compound remaining: 25% (*d*PB) and 15% (*d*PE) in the rat vs. 51% (*d*PB) and 41% (*d*PE) in human). *d*PB produced eight metabolites (B1–B8) in RLMs and nine metabolites (B1–B9) in HLMs. *d*PE formed 13 identical metabolites in both species. Further, the relative ratios of the metabolites, as calculated based on the peak area ratio of each metabolite to that of B1 or E1 formed from *d*PB or *d*PE in RLMs, were different in rats and humans (Fig. 10). B3, one of the metabolites generated from hydrolysis of one angeloyl group from the C-3′ position of *d*PB, was the most abundant metabolite in RLMs while B3 and B8, the metabolites generated via mono-oxidation on the C-4′ side chain of *d*PB, were two major metabolites in HLMs. (−)-*cis*-Khallectone (B1), formed from loss of both angeloyl moieties from the C-3′ and C-4′ positions, was less than one-tenth of B3 in both species. In *d*PE metabolism, the metabolite formed via hydrolysis ((−)-*cis*-khallectone (E1)), has the highest relative ratio in RLMs, while the metabolite

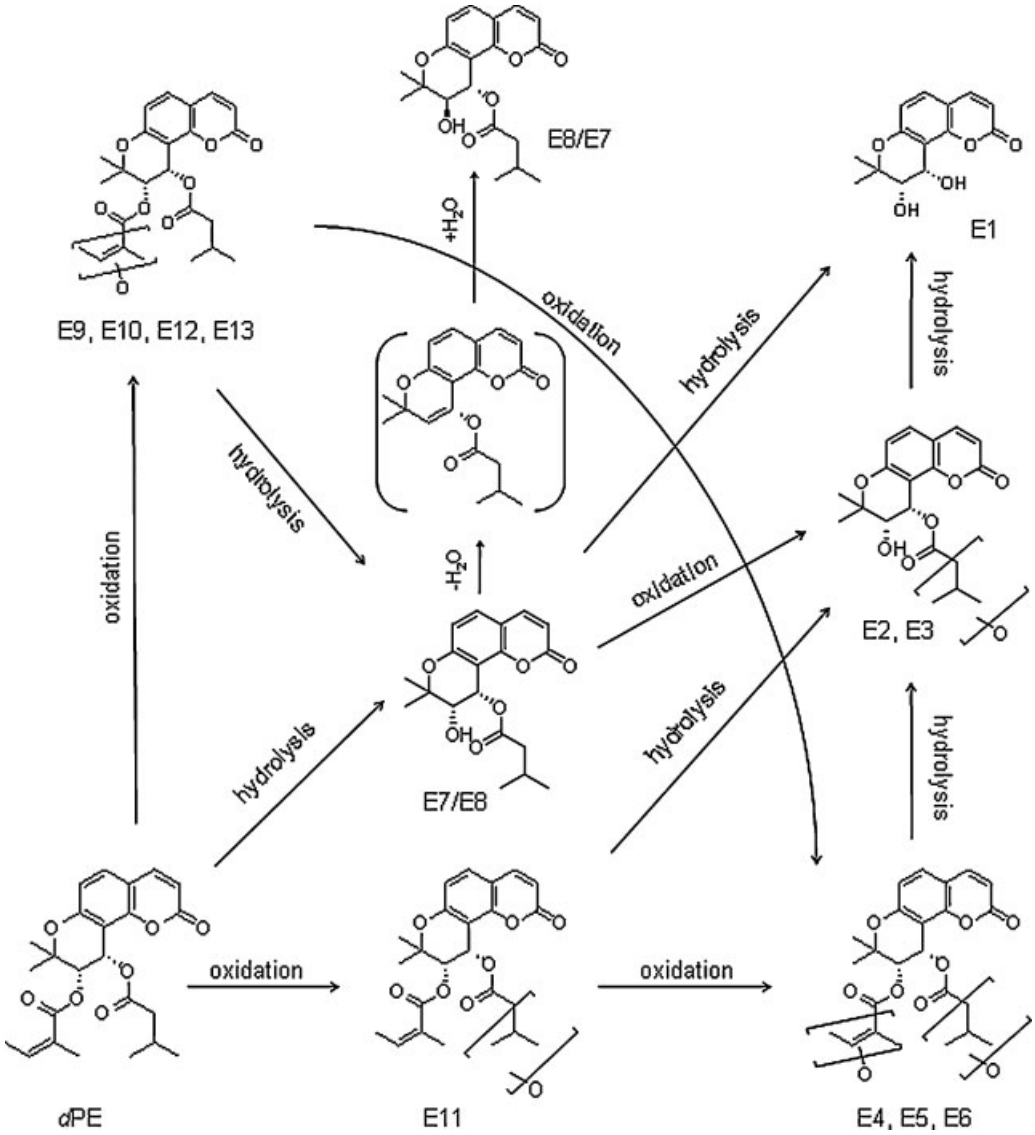

Figure 9. Proposed metabolic pathways of *d*PE in liver microsomes of rats and humans. The intermediate is shown in brackets.

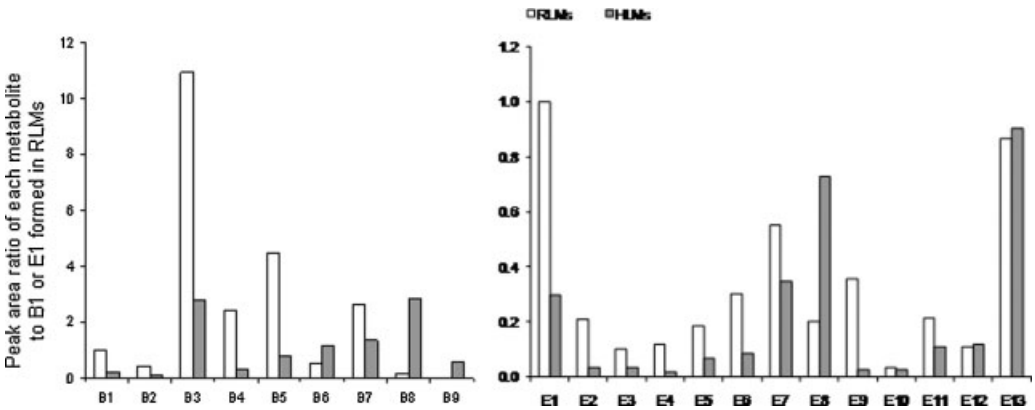

Figure 10. Relative ratios of the metabolites of *d*PB (left) and *d*PE (right) produced in liver microsomal proteins of rats and humans.

formed from mono-oxidation (E13) predominated in HLMs (Fig. 10). The species difference could be attributed to the well-characterized species difference in CYP450 expression between rats and humans.[30,31]

CONCLUSIONS

This is the first report on *d*PB and *d*PE metabolisms in rat and human liver microsomes. The metabolites were tentatively identified using liquid chromatography coupled with electrospray tandem mass spectrometry and time-of-flight mass spectrometry. The ESI-MS^n fragmentation profiles of *d*PE and its metabolites followed the same pathway as those of the angular-type pyranocoumarins from Peucedani Radix reported previously, thus might aid identification of other pyranocoumarins and metabolites based on their sequential mass fragmentation profiles. The current results have also demonstrated that HPLC/IT-MS/MS coupling with HPLC/TOF-MS is a rapid, sensitive and reliable tool for the characterization of unknown metabolites in biological samples. Oxidation and hydrolysis were proved to be the two predominant pathways of both compounds and substituents at the C-3′ and C-4′ positions determine the extent and the type of reactions. Furthermore, species difference in *d*PB and *d*PE biotransformation was insignificant, supporting the rat as a suitable substitute for predicting the metabolic profile of *d*PB and *d*PE in human. Further studies are ongoing in our laboratory on identification of the main CYP450 isozyme(s) involved and the *in vivo* metabolic profiles of *d*PB and *d*PE.

Acknowledgements

The research was supported by the National Basic Research Program of China (973 program, Grant No. 2009CB522707) and the Research Committee of University of Macau (Project No. UL016/09-Y1/CMSWYT01/ICMS).

REFERENCES

[1] The State Pharmacopoeia Commission of P.R. China. Peucedani Radix, in *Pharmacopoeia of the People's Republic of China*, vol. I, Chemical Industry Press, Beijing, **2010**, p. 248.
[2] S. C. Xi, Y. M. Ruan, L. Z. Zhang. *Zhongguo Zhong Xi Yi Jie He Za Zhi*. **1996**, *16*, 218.
[3] R. Zhou, H. L. Wang, X. H. Zhang, J. Xing, C. M. Li. *Zhongguo Yi Ke Da Xue Xue Bao* **2001**, *30*, 325.
[4] N. C. Zhao, H. L. Wang, X. Jin, X. H. Zhang, K. J. Liu, F. L. Guan. *Zhongguo Yi Ke Da Xue Xue Bao* **1994**, *23*, 197.
[5] J. Kang, R. J. Yu. *Zhongguo Yi Ke Da Xue Xue Bao* **1994**, *23*, 122.
[6] Q. Y. Wang, E. R. Li, G. X. Zhao, J. Kang, X. M. Hou, R. J. Yu. *Zhongguo Yi Ke Da Xue Xue Bao* **1998**, *27*, 588.
[7] Z. X. Chen, B. S. Huang, Q. L. She, G. F. Zeng. *Acta Pharm. Sin.* **1979**, *14*, 486.
[8] J. S. Ye, H. Q. Zhang, C. Q. Yuan. *Acta Pharm. Sin.* **1982**, *17*, 431.
[9] H. T. Chang, Y. Okada, T. Okuyama, P. F. Tu. *Magn. Reson. Chem.* **2007**, *45*, 611.
[10] H. T. Chang, Y. Okada, T. J. Ma, T. Okuyama, P. F. Tu. *J. Asian Nat. Prod. Res.* **2008**, *10*, 577.
[11] J. Y. Wu, W. F. Fong, J. X. Zhang, C. H. Leung, H. L. Kwong, M. S. Yang, D. Li, H. Y. Cheung. *Eur. J. Pharmacol.* **2003**, *473*, 9.
[12] Y. Aida, T. Kasama, N. Takeuchi, S. Tobinaga. *Chem. Pharm. Bull.* **1995**, *43*, 859.
[13] Z. Xu, X. Wang, Y. Dai, L. Kong, F. Wang, H. Xu, D. Lu, J. Song, Z. Hou. *Chem. Biol. Interact.* **2010**, *186*, 239.
[14] M. R. Rao, W. B. Liu, P. Q. Liu. *Acta Pharm. Sin.* **2001**, *36*, 165.
[15] N. C. Zhao, W. B. Jin, X. H. Zhang, F. L. Guan, Y. B. Sun, H. Adachi, T. Okuyama. *Biol. Pharm Bull.* **1999**, *22*, 984.
[16] M. Yoshikawa, N. Nishida, K. Ninomiya, T. Ohgushi, M. Kubo, M. Toshio, H. Matsuda. *Bioorg. Med. Chem.* **2006**, *14*, 456.
[17] W. Chan, L. Cui, G. W. Xu, Z. W. Cai. *Rapid Coummun. Mass Spectram.* **2006**, *20*, 1775.
[18] J. F. Garda-Reyes, I. Ferrer, E. M. Thurman, A. Molina-Diaz, A. R. Fernandez-Alba. *Rapid Commun. Mass Spectram.* **2005**, *19*, 2780.
[19] H. Nishino, T. Okuyama, M. Takata, S. Shibata, H. Tokuda, J. Takayasu, T. Hasegawa, A. Nishino, H. Ueyama, A. Iwashima. *Carcinogenesis* **1990**, *11*, 1557.
[20] X. D. Wu, X. Wu. *Chin. Pharm. J.* **1996**, *31*, 234.
[21] G. Lin, J. Tang, X. Q. Liu, Y. Jiang, J. Zheng. *Drug Metab. Dispos.* **2007**, *35*, 607.
[22] O. H. Lowry, N. J. Rosenbrough, A. L. Farr, R. J. Randall. *J. Biol. Chem.* **1951**, *193*, 265.
[23] X. L. Wu, L. Y. Kong, Z. D. Min. *Acta Pharm. Sin.* **2002**, *37*, 527.
[24] Y. Tao, J. Luo, Y. Lu, D. Xu, Z. Hou, L. Y. Kong. *Nat. Prod. Commun.* **2009**, *4*, 1079.
[25] G. Y. Zhu, G. Y. Chen, Q. Y. Li, X. L. Shen, H. X. Fang. *Chin. J. Nat. Med.* **2004**, *2*, 308.
[26] M. Suzuki, Y. Li, P. C. Smith, J. A. Swenberg, D. E. Martin, S. L. Morris-Natschke, K. H. Lee. *Drug Metab. Dispos.* **2005**, *33*, 1588.
[27] Z. Sun, D. J. Murry, S. P. Sanghani, W. I. Davis, N. Y. Kedishvili, Q. Zou, T. D. Hurley, W. F. Bosron. *JPET* **2004**, *310*, 469.
[28] Q. G. Zhu, J. H. Hu, H. W. Zeng. *Acta Pharmaceutica Sinica* **2005**, *40*, 322.
[29] Y. Yoshigae, T. Imai, M. Taketani, M. Otagiri. *Chirality* **1999**, *11*, 10.
[30] D. F. Lewis, C. Ioannides, D. V. Parke. *Environ. Health Perspect.* **1998**, *106*, 633.
[31] M. Turpeinen, C. Ghiciuc, M. Opritoui, L. Tursas, O. Pelkonen, M. Pasanen. *Xenobiotica* **2007**, *37*, 1367.

